JOC The Journal of Organic Chemistry

Article

pubs.acs.org/joc

Time-Resolved Infrared (TRIR) Studies of Oxycarbonylnitrenes

Tyler A. Chavez, Yonglin Liu, and John P. Toscano*

Department of Chemistry, Johns Hopkins University, Baltimore, Maryland 21218, United States

Supporting Information

ABSTRACT: *N*-Ethyloxycarbonyl-*S*,*S*-dibenzothiphene sulfilimine and *N*-*t*-butyloxycarbonyl-*S*,*S*-dibenzothiphene sulfilimine have been utilized as precursors to ethoxycarbonylnitrene and *t*-butyloxycarbonylnitrene. B3LYP/6-31G(d) calculations predict triplet ground states for both oxycarbonylnitrenes, albeit by small margins. Triplet ethoxycarbonylnitrene and triplet *t*-butyloxycarbonylnitrene have been observed following photolysis of these sulfilimine precursors by time-resolved infrared (TRIR) spectroscopy. Kinetic studies show that ethoxycarbonylnitrene reacts with solvents such as acetonitrile and cyclohexane, while *t*-butyloxycarbonylnitrene undergoes an intramolecular insertion reaction to produce 5,5-dimethyl oxazolidinone. Product analysis following photolysis of *N*-*t*-butyloxycarbonyl-*S*,*S*-dibenzothiphene sulfilimine confirms that the oxazolidinone is the major product with an estimated yield of 90%. The products from these two nitrenes are derived from the corresponding singlet nitrene, either directly or via thermal repopulation of the singlet from the lower-energy triplet nitrene.

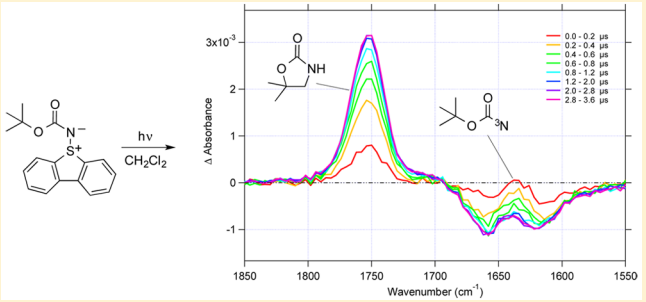

INTRODUCTION

Oxycarbonylnitrenes (ROC(O)N) have a rich history in the development of our modern mechanistic understanding of nitrene chemistry.[1] Seminal studies by Lwowski and co-workers on ethoxycarbonylazide (**1**) demonstrated ethoxycarbonylnitrene (**2**) undergoes intermolecular insertion reactions into C−H bonds and adds to double bonds with partial stereospecificity that suggested reaction from both singlet **2s** and presumably lower-energy triplet nitrene **2t** (Scheme 1).[2−5] Similar work in

Scheme 1

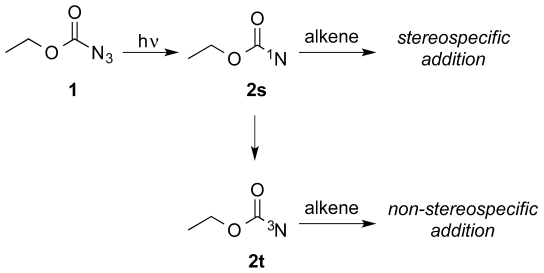

Germany also demonstrated that photochemical decomposition of *t*-butyloxycarbonylazide (**3**) produces *t*-butyloxycarbonylnitrene (**4**) that predominantly gives 5,5-dimethyl-2-oxazolidinone (**5**) via an intramolecular C−H insertion reaction in a variety of solvents (Scheme 2).[6−8] More recent synthetic and spectroscopic studies on oxycarbonylnitrenes have confirmed the above reactivity and provided additional insight into these interesting reactive intermediates.[9−12]

Lwowski and co-workers were also the first to suggest that the classic photo-Curtius rearrangement of acyl azides to isocyanates

Scheme 2

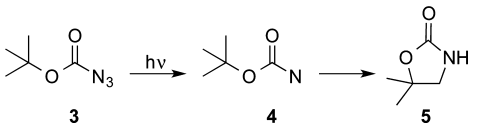

does not occur from the nitrene intermediate, but rather directly from the azide.[13−15] Subsequent low-temperature matrix infrared and solution nanosecond time-resolved infrared (TRIR) spectroscopic studies confirmed that the isocyanate is not formed from a relaxed nitrene intermediate.[16−18] Recently, ultrafast IR and UV−vis studies of Platz and co-workers have provided spectroscopic evidence for this pathway, demonstrating directly that the first singlet excited state (S_1) of the acyl azide is the isocyanate precursor.[19−22]

Low-temperature ESR spectroscopic studies confirmed the suspected triplet ground state for ethoxycarbonylnitrene and related species,[23] consistent with the observed nonstereospecific trapping of alkenes. These observations are in contrast to those found for carbonylnitrenes (RC(O)N), which have been shown to be ground state singlets that are not detectable by ESR spectroscopy and show retention of configuration upon addition to alkenes.[10,24]

The singlet and triplet state structures and energies of both oxycarbonyl- and carbonylnitrenes have been thoroughly investigated by computational methods, which provide insight into their different ground states.[11,18,25−29] High-level theory indicates that carbonylnitrenes are closed-shell ground state

Received: April 26, 2016
Published: June 30, 2016

ACS Publications © 2016 American Chemical Society

DOI: 10.1021/acs.joc.6b00949
J. Org. Chem. 2016, 81, 6320−6328

singlets due to a significant bonding interaction between a carbonyl oxygen lone pair and an empty orbital on the nitrene nitrogen.[18,26−29] Indeed, computed structures of singlet carbonylnitrenes have significant cyclic oxazirene character (Figure 1).

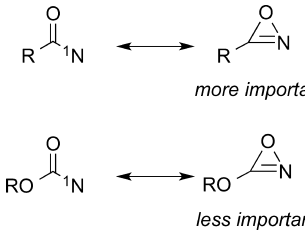

Figure 1. Relevant resonance structures for carbonyl- and oxycarbonylnitrenes.

Oxycarbonylnitrenes, on the other hand, are computed to be ground state triplets since this oxazirene stabilization is now less important (Figure 1) and oxygen conjugation into the carbonyl stabilizes the triplet more than the corresponding closed-shell singlet state.[27,28] Inductive effects have also been suggested to play a role in reducing the stabilization of the singlet by limiting the carbonyl oxygen's nucleophilicity/basicity, as well as by increasing the O−C−N bond angle in accord with Bent's rule.[30−32]

Although standard B3LYP/6-31G(d) calculations give optimized geometries for oxycarbonyl- and carbonylnitrenes in very good agreement with those calculated by higher levels of theory (CCSD(T) with complete basis set extrapolation or CBS-QB3 calculations), singlet−triplet energy gaps ($\Delta E_{ST} = E_S - E_T$) are overestimated.[18,27,28] For example, B3LYP/6-31G(d) calculations overestimate ΔE_{ST} by approximately 9 kcal/mol for formylnitrene (HC(O)N) and approximately 7 kcal/mol for carboxynitrene (HOC(O)N).[28]

To gain additional insight into the chemistry and reactivity of oxycarbonylnitrenes, we are pleased to report herein nanosecond TRIR studies of ethoxycarbonylnitrene (**2**) and *t*-butyloxycarbonylnitrene (**4**) in a variety of solvents. Although azides are standard photoprecursors for nitrenes, recent work has demonstrated that these intermediates also can be efficiently generated from analogous sulfilimine precursors.[29,33−36] Thus, we have utilized the sulfilimine photoprecursors **6** and **7** for these studies (Figure 2).

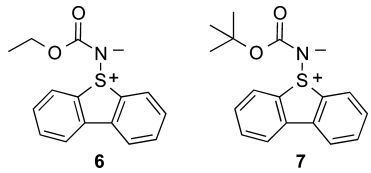

Figure 2. Sulfilimine-based photoprecursors to oxycarbonylnitrenes **2** and **4**.

RESULTS AND DISCUSSION

Computational Studies. The B3LYP/6-31G(d) calculated ΔE_{ST} values of the *syn*- and *anti*-rotamers of ethoxycarbonylnitrene (**2**) are 12.8 and 8.8 kcal/mol, respectively, and 13.1 and 9.3 kcal/mol, respectively, with the inclusion of zero-point vibrational energy correction (Figure 3a). Given that B3LYP/6-31G(d) calculations overestimates the ΔE_{ST} of carboxynitrene (HOC(O)N) by 7 kcal/mol,[28] we estimate that the ΔE_{ST} values

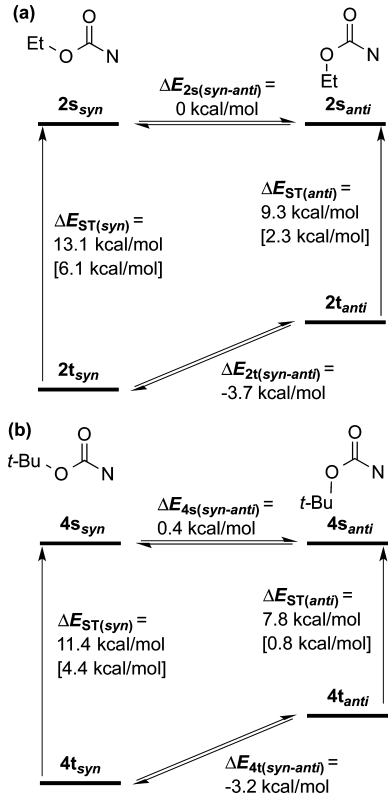

Figure 3. B3LYP/6-31G(d) calculated ΔE_{ST} values ($\Delta E_{ST} = E_S - E_T$) and relative energies of the *syn*- and *anti*-forms, including zero-point vibrational energy correction, of (a) ethoxycarbonylnitrene (**2**) and (b) *t*-butoxycarbonylnitrene (**4**). Values in brackets include the 7 kcal/mol correction to the B3LYP/6-31G(d) values.[28]

of the *syn*- and *anti*-rotamers of ethoxycarbonylnitrene (**2**) are 6.1 and 2.3 kcal/mol, respectively (Figure 3a). Similar to HOC(O)N,[28] the *syn*- and *anti*-rotamers of singlet nitrene **2s** are very close in energy, but the *syn*-rotamer of triplet nitrene **2t** is 3.7 kcal/mol lower in energy than the corresponding *anti*-rotamer (Figure 3a). The barrier to rotation from *syn*- to *anti*-forms of **2s** is calculated to be 6.1 kcal/mol, while that of triplet **2t** is higher, 9.4 kcal/mol, presumably the result of a larger O−C−N bond angle (see below).

In comparison, the B3LYP/6-31G(d) calculated ΔE_{ST} values of the *syn*- and *anti*-rotamers of *t*-butyloxycarbonylnitrene (**4**) were found to be 11.0 and 7.2 kcal/mol, respectively, and 11.4 and 7.8 kcal/mol, respectively, with the inclusion of zero-point vibrational energy correction. Taking into account the 7 kcal/mol B3LYP/6-31G(d) correction,[28] the ΔE_{ST} values of the *syn*- and *anti*-rotamers of *t*-butoxycarbonylnitrene are estimated to be 4.4 and 0.8 kcal/mol, respectively (Figure 3b). These ΔE_{ST} values match well with CBS-QB3 calculated values for methoxycarbonylnitrene that have been previously reported.[27]

As with ethoxycarbonylnitrene, the *syn*- and *anti*-rotamers of singlet nitrene **4s** are very close in energy, while the *syn*- and *anti*-rotamers of triplet nitrene **4t** are separated by 3.2 kcal/mol in favor of the *syn*-form (Figure 3b). The B3LYP/6-31G(d) calculated barriers to rotation from the *syn*- to *anti*-form of **4s** is calculated to be 4.7 kcal/mol, while that for triplet **4t** is 7.5 kcal/mol (Supporting Information).

Analysis of the B3LYP/6-31G(d) calculated geometries of both ethoxy- and *t*-butoxycarbonylnitrene show a contribution from the oxazirine resonance form in the singlet states of both

DOI: 10.1021/acs.joc.6b00949
J. Org. Chem. 2016, 81, 6320−6328

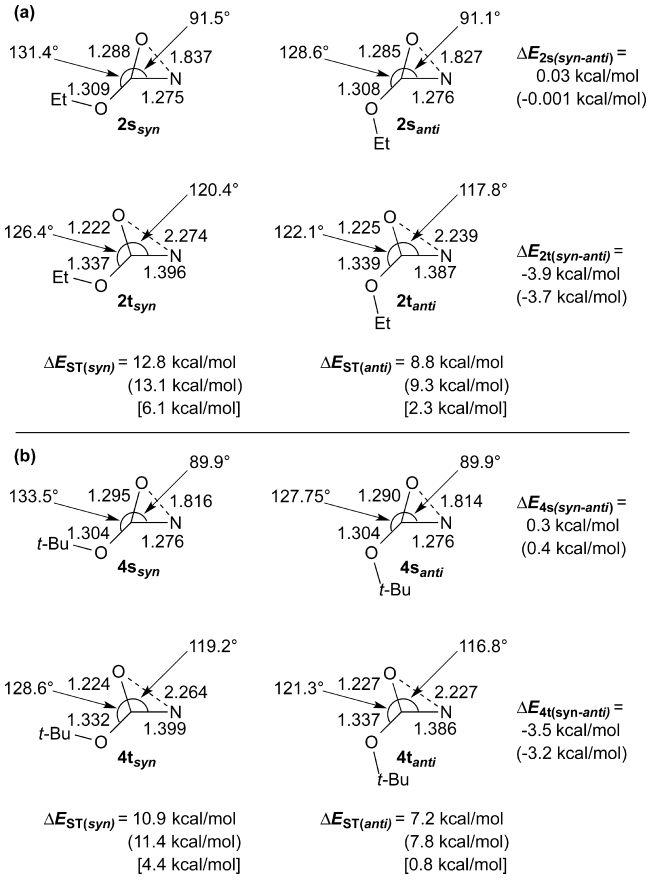

Figure 4. B3LYP/6-31G(d) calculated geometries and energies of both *syn*- and *anti*-forms of (a) ethoxycarbonylnitrene (**2**) and (b) *t*-butoxycarbonylnitrene (**4**). Energies shown in parentheses include zero-point vibrational energy correction. Values in brackets include the 7 kcal/mol correction to the B3LYP/6-31G(d) values.

nitrenes. This effect is reflected in the significantly smaller O−C−N bond angles of 91.5° and 91.1° in *syn*- and *anti*-singlet **2s**, respectively, relative to 120.4° and 117.8° for *syn*- and *anti*-triplet **2t**, respectively (Figure 4a). The same effect is also observed for *t*-butoxycarbonylnitrene, with O−C−N bond angles of 89.9° for both the *syn*- and *anti*-forms of singlet **4s**, while *syn*- and *anti*-triplet **4t** have calculated angles of 119.2° and 116.8°, respectively. However, the calculation of triplet ground states for these nitrenes suggests a less important role of this resonance form compared to that in carbonylnitrenes.[30−32]

Significant differences in the geometries of the two nitrene spin states result in considerably different IR signatures. The singlet nitrenes are calculated to have strong C−O stretching vibrations at ca. 1750 cm^{-1}, while the C−O stretch in the triplets is calculated to appear at ca. 1605 cm^{-1} (scaled by 0.96).[37] Therefore, both singlet and triplet oxycarbonylnitrenes can be distinguished by their frequencies in solution if their lifetimes are sufficiently long enough. Previous TRIR work on other carbonylnitrenes has shown that they can be detected in solution at frequencies similar to those calculated.[29,33,38]

Time-Resolved IR Studies of Ethoxycarbonylnitrene (2). Upon 266 nm laser photolysis of sulfilimine **6** in argon-saturated acetonitrile (CH_3CN), the TRIR difference spectrum shown in Figure 5 is observed. The transient species observed at 1640 cm^{-1}, which overlaps with a sulfilimine depletion band, decays with an observed first-order rate of 5.5 × 10^5 s^{-1} (Figure 6a). Photolysis in oxygen-saturated acetonitrile does not affect the rate of decay of this signal. Platz and Buron detected triplet ethoxycabonylnitrene (**2t**) upon photolysis of carboethoxyazide (**1**), and did not observe reactivity with O_2.[11] We assign the observed 1640 cm^{-1} TRIR signal to *syn*-triplet ethoxycarbonylnitrene (*syn*-**2t**), which is a reasonable match with its calculated frequency (1605 cm^{-1}). In comparison, the calculated IR frequency of *syn*-singlet ethoxycarbonylnitrene (*syn*-**2s**) is 1752 cm^{-1}. Similar to results from previous work,[11] the lifetime of the 1640 cm^{-1} signal is shortened in the presence of the H atom donor triethylsilane (TES), further suggesting that the triplet nitrene is responsible for this signal (Supporting Information).

Triplet nitrene **2t** decays at the same rate as the growth of signals at 1690, 1285, and 1160 cm^{-1} (Figure 6). We assign these

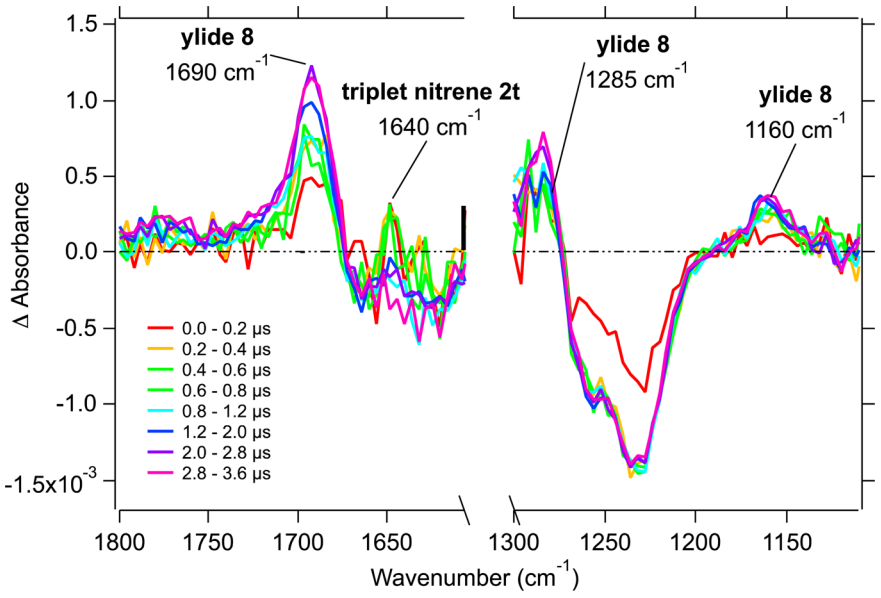

Figure 5. TRIR difference spectra averaged over the indicated time scales following 266 nm laser photolysis of sulfilimine **6** (3 mM) in argon-saturated acetonitrile. The black bar reflects the B3LYP/6-31G(d) calculated frequency of *syn*-triplet ethoxycarbonylnitrene (*syn*-**2t**).

DOI: 10.1021/acs.joc.6b00949
J. Org. Chem. 2016, 81, 6320−6328

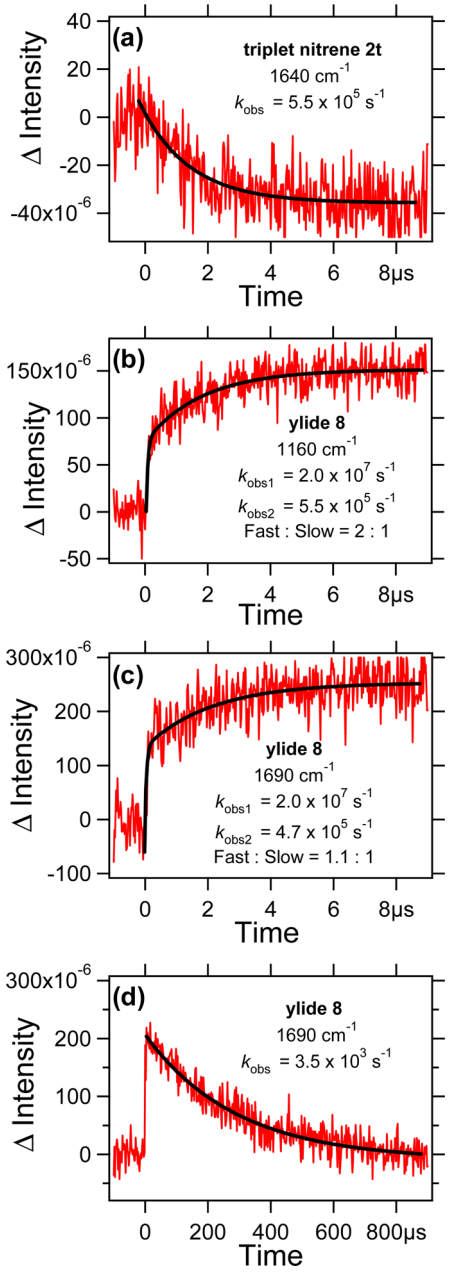

Figure 6. Kinetic traces observed following 266 nm laser photolysis of sulfilimine **6** in argon-saturated acetonitrile at (a) 1640 cm^{-1} from −1 to 9 μs, (b) 1160 cm^{-1} from −1 to 9 μs, (c) 1690 cm^{-1} from −1 to 9 μs, and (d) 1690 cm^{-1} from −100 to 900 μs. Black curves are the calculated best fit to a single- or double-exponential function.

Scheme 3

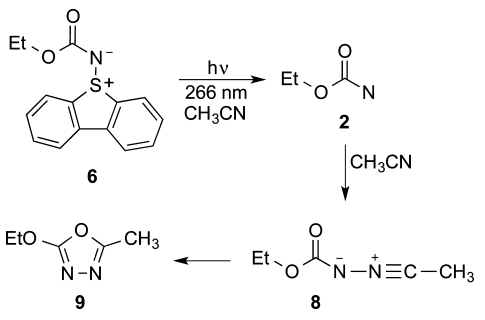

IR bands to ylide **8**, the product of reaction of the nitrene with acetonitrile (Scheme 3). The observed rate of ylide growth fits well to a biexponential function, indicative of kinetics composed of a fast component, produced within the instrumental time resolution ($k = 2 \times 10^7$ s^{-1}), and a slower, resolvable component ($k = 5.5 \times 10^5$ s^{-1}). The slow component of the ylide growth matches the decay of the triplet nitrene, indicating that this portion of the observed kinetics is due to **2t**, although carbonylnitrene reactivity with acetonitrile has typically been associated with the singlet. The fast component is likely the result of reactivity of the singlet nitrene **2s**, consistent with the reported growth of **2s** within 10 ns in Freon-113 by Platz and Buron.[11] The ylide further decays with an observed first-order rate of 3.5×10^5 s^{-1} to produce oxadiazole **9** (Scheme 3), which is confirmed by ^{1}H NMR spectroscopic analysis of the reaction (Supporting Information).

Upon 266 nm laser photolysis of sulfilimine **6** in argon-saturated cyclohexane, the TRIR difference spectrum shown in Figure 7 is observed. Analogous to TRIR experiments in acetonitrile, we detect **2t** at 1640 cm^{-1} (Figures 7 and 8a). Here, the product of reaction with solvent is presumably amide **10** (Scheme 4), as has been observed in related work.[33,39] The triplet nitrene decays ($k = 7.1 \times 10^5$ s^{-1}) at the same rate as the growth of the slow component of amide **10**, which is observed at 1728 cm^{-1}, in excellent agreement with its reported frequency (1730 cm^{-1}).[40] We also observe a fast component for the growth of the 1728 cm^{-1} signal, suggesting reactivity from singlet nitrene **2s** (Figure 8b). In addition, we observe a very weak positive band at 2180 cm^{-1}, produced within the instrumental time resolution (Figure 8c). This species is assigned to ethoxyisocyanate (**11**, Scheme 4), which is in reasonable agreement with the reported literature frequency of 2204 cm^{-1}. Since this species is formed within the instrumental time resolution (50 ns), the source of the isocyanate is likely either an excited state of precursor **6** or singlet nitrene **2s** (Scheme 4).

Time-Resolved IR Studies of t-Butyloxycarbonylnitrene (4). Upon 266 nm laser photolysis of sulfilimine **7** in argon-saturated acetonitrile, the TRIR difference spectrum shown in Figure 9 is observed. Triplet nitrene **4t** is detected at 1640 cm^{-1} (Figures 9 and 10a); however, in contrast to the chemistry observed with nitrene **2** in acetonitrile, formation of the corresponding acetonitrile ylide is not observed. Triplet nitrene **4t** instead decays at the same observed rate as the growth of an intense signal at 1762 cm^{-1} (Figures 9 and 10b). This 1762 cm^{-1} band matches reasonably well with the reported literature frequency of oxazolidinone **5** (1740 cm^{-1}),[41] formed via an intramolecular C−H insertion reaction (Scheme 5). ^{1}H NMR product analysis following 254 nm photolysis in both acetonitrile-d_3 and dichloromethane-d_2, confirms the production of **5** in ca. 90% yield (Supporting Information). The growth of oxazolidinone **5** displays biexponential kinetics (Figure 10b) with the fast component presumably due to production from singlet nitrene **4s**. We also observe the production of *t*-butoxyisocyante (**12**) at 2180 cm^{-1}, which grows within the instrumental time resolution (Figure 10c).

Laser photolysis of sulfilimine **7** in argon-saturated dichloromethane results in the TRIR difference spectrum shown in Figure 11. Again, we observe triplet nitrene **4t** and oxazolidinone **5** at 1638 and 1752 cm^{-1}, respectively. Rapid production of isocyanate **12** is also observed at 2175 cm^{-1} (Figure 12). Interestingly, the ratio of fast component to slow component for growth of oxazolidinone **5** in dichloromethane (1:1.4, Figure 12b) is significantly different from that observed in acetonitrile

DOI: 10.1021/acs.joc.6b00949
J. Org. Chem. 2016, 81, 6320−6328

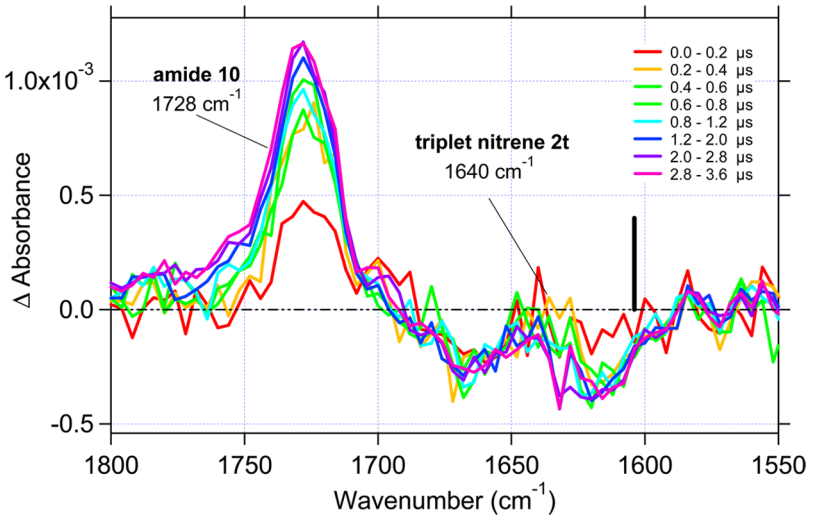

Figure 7. TRIR difference spectra averaged over the indicated time scales following 266 nm laser photolysis of sulfilimine **6** (3 mM) in argon-saturated cyclohexane. The black bar reflects the B3LYP/6-31G(d) calculated frequency of *syn*-triplet ethoxycarbonylnitrene (*syn*-**2t**).

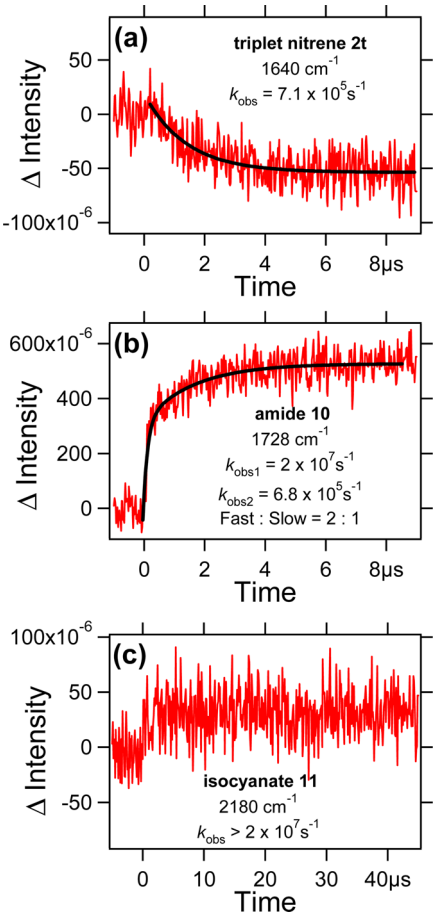

Figure 8. Kinetic traces observed following 266 nm laser photolysis of sulfilimine **6** in argon-saturated cyclohexane at (a) 1640 cm^{-1} from −1 to 9 μs, (b) 1728 cm^{-1} from −1 to 9 μs, and (c) 2180 cm^{-1} from −5 to 45 μs. Black curves are the calculated best fit to a single- or double-exponential function.

(9:1, Figure 10b). TRIR experiments in Freon-113 reveal analogous signals (Figure 13). In this solvent, the ratio of fast to slow component for the growth of oxazolidinone **5** is now 1:1.3 (Figure 14b). The greater contribution of the fast component to

Scheme 4

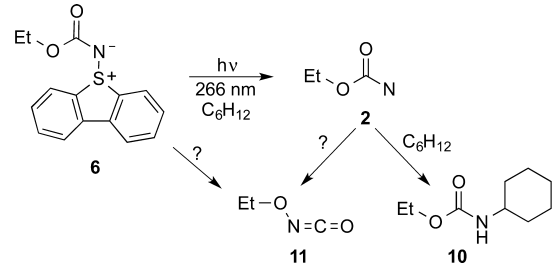

the observed oxazolidinone growth kinetics in acetonitrile (dielectric constant, ε = 35.9) compared to that in either dichloromethane (ε = 8.9) or Freon-113 (ε = 2.4) suggests a solvent effect on the relative stabilities of the singlet and triplet states of nitrene **4** and/or on the reactions involved in oxazolidinone formation.

This solvent effect is reminiscent of our previous TRIR studies of carbonylcarbenes where singlet carbonylcarbenes were found to be favored in polar solvents, the result of their increased dipole moment.[42,43] The singlet and triplet carbonylcarbenes in these previous studies were in rapid equilibrium, with distinct TRIR bands displaying identical kinetics. In contrast, we find no evidence that singlet **4s** and triplet **4t** are in rapid equilibrium. Indeed, we do not observe singlet **4s** in our TRIR experiments, and the observed growth kinetics of product **5** indicate a separate kinetic contribution from the singlet nitrene (fast) and the triplet nitrene (slow). These observed growth kinetics may be explained by two potential mechanisms: (1) separate production of **5** from singlet **4s** and triplet **4t** (Scheme 6a) or (2) production of **5** from only singlet **4s**, with the slow component being the result of thermal repopulation of **4s** from **4t** (Scheme 6b). These mechanisms may also similarly account for the observed growth kinetics of ylide **8** (Figure 6b,c) and amide **10** (Figure 8b).

Given that ylide formation is expected to be a singlet nitrene reaction, we propose that the mechanism shown in Scheme 6b is operative for formation of ylide **8**, as well as oxazolidinone **5** and amide **10**. B3LYP/6-31(d) analysis of the reaction between triplet nitrene **2t** and acetonitrile is also consistent with this proposal (Supporting Information). The initial triplet biradical formed in this reaction is calculated to be 48 kcal/mol higher in

DOI: 10.1021/acs.joc.6b00949
J. Org. Chem. 2016, 81, 6320−6328

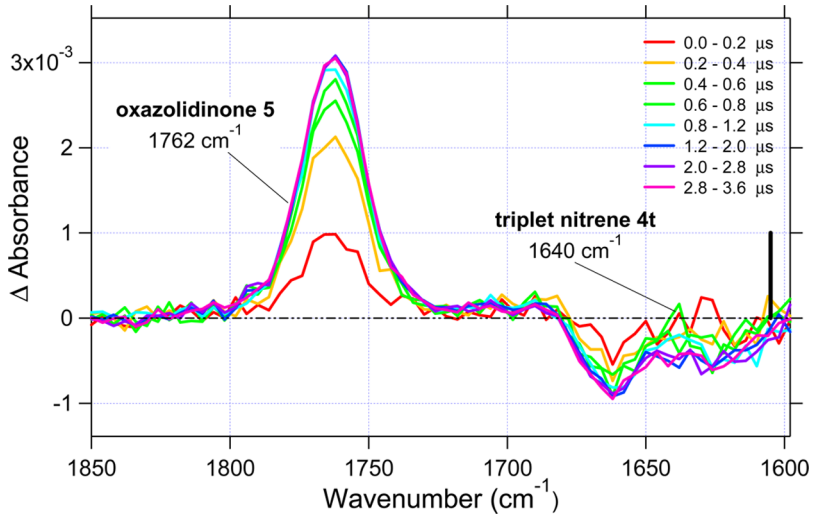

Figure 9. TRIR difference spectra averaged over the indicated time scales following 266 nm laser photolysis of sulfilimine **7** (3 mM) in argon-saturated acetonitrile. The black bar reflects the B3LYP/6-31G(d) calculated frequency of *syn*-triplet *t*-butyloxycarbonylnitrene (*syn*-**4t**).

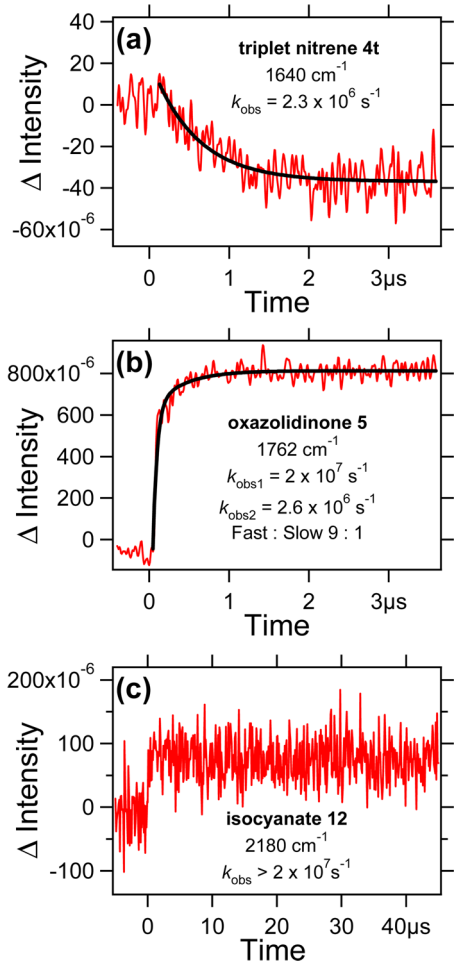

Figure 10. Kinetic traces observed following 266 nm laser photolysis of sulfilimine **7** in argon-saturated acetonitrile at (a) 1640 cm^{-1} from −0.4 to 3.6 μs, (b) 1762 cm^{-1} from −0.4 to 3.6 μs, and (c) 2180 cm^{-1} from −5 to 45 μs. Black curves are the calculated best fit to a single- or double-exponential function.

energy than ylide **8**. Moreover, the reaction of triplet **2t** with acetonitrile to form the triplet biradical is thermodynamically uphill by ca. 12 kcal/mol, whereas the reaction of singlet nitrene **2s** plus acetonitrile to form ylide **8** is thermodynamically downhill by ca. 46 kcal/mol.

Scheme 5

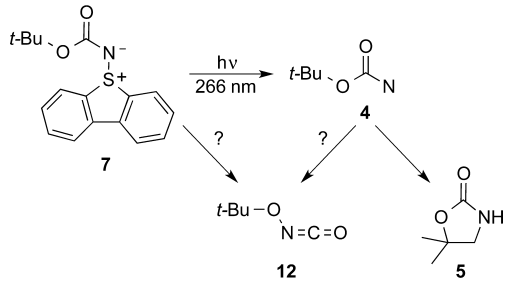

CONCLUSIONS

N-Substituted dibenzothiophene sulfilimine-based precursors are efficient photoprecursors to ethoxycarbonylnitrene and *t*-butyloxycarbonylnitrene. Computational analysis indicates that both of these nitrenes are ground state triplets, albeit by small margins. TRIR spectroscopy was used to detect triplet ethoxycarbonylnitrene and triplet *t*-butyloxycarbonylnitrene in several solvents. Ethoxycarbonylnitrene reacts with acetonitrile to form an ylide and with cyclohexane to form an amide. Conversely, *t*-butyloxycarbonylnitrene exclusively forms an intramolecular C−H insertion oxazolidinone product, independent of solvent. The observed product growth kinetics for the ylide, amide, and oxazolidinone suggest a contribution from both the corresponding triplet (slow) and singlet (fast) nitrene. On the basis of the observed TRIR data, B3LYP calculations, and expected nitrene reactivity, we conclude that these products are formed from the corresponding singlet nitrene, either directly (fast kinetic contribution) or via thermal repopulation of the singlet from the lower-energy triplet nitrene (slow kinetic contribution).

EXPERIMENTAL METHODS

General Methods. Unless otherwise noted, materials were used without further purification. High-resolution mass spectra were obtained on a magnetic sector mass spectrometer operating in fast atom bombardment ionization mode. Masses were referenced to a 10% PEG-200 sample.

DOI: 10.1021/acs.joc.6b00949
J. Org. Chem. 2016, 81, 6320−6328

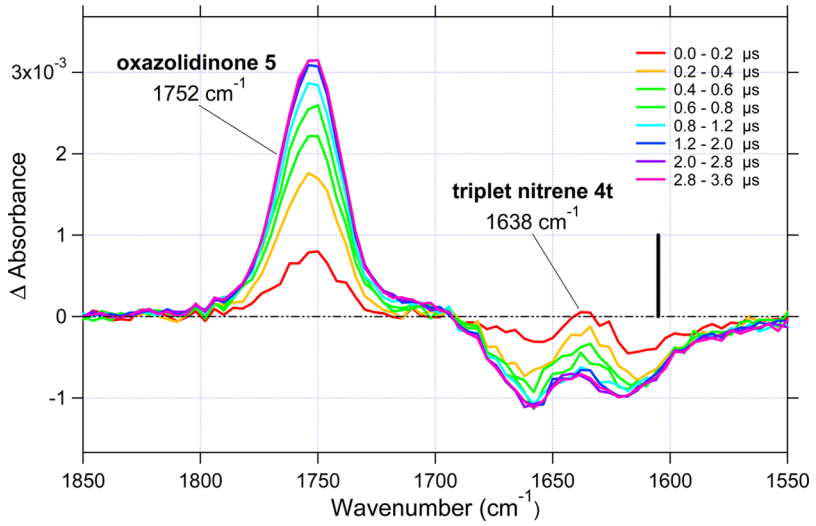

Figure 11. TRIR difference spectra averaged over the indicated time scales following 266 nm laser photolysis of sulfilimine **7** (3 mM) in argon-saturated dichloromethane. The black bar reflects the B3LYP/6-31G(d) calculated frequency of *syn*-triplet *t*-butyloxycarbonylnitrene (*syn*-**4t**).

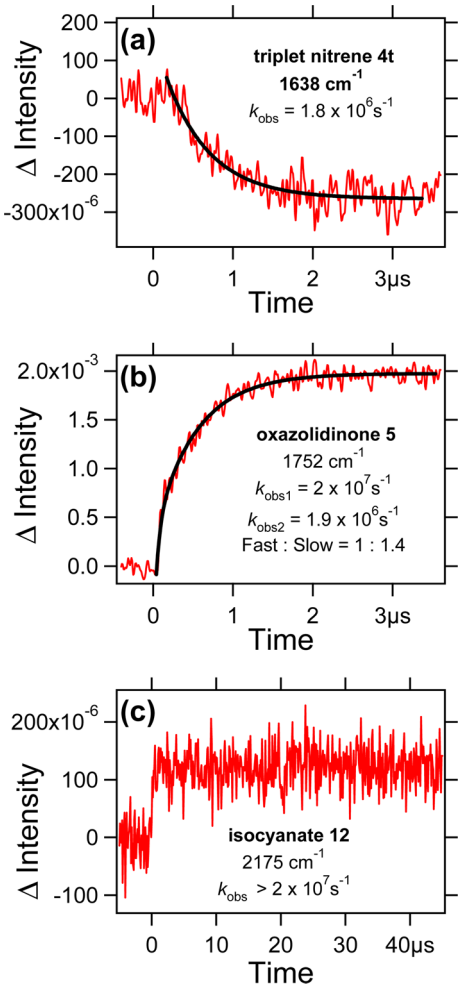

Figure 12. Kinetic traces observed following 266 nm laser photolysis of sulfilimine **7** in argon-saturated dichloromethane at (a) 1638 cm^{-1} from −0.4 to 3.6 μs, (b) 1752 cm^{-1} from −0.4 to 3.6 μs, and (c) 2175 cm^{-1} from −5 to 45 μs. Black curves are the calculated best fit to a single- or double-exponential function.

*N-Ethoxycarbonyl Dibenzothiophene Sulfilimine (**6**).* This compound was prepared by two methods. Method A is analogous to that reported by Nakayama and co-workers.[44] Dibenzothiophene *S*-oxide (0.350 g, 1.75 mmol) in dichloromethane (10 mL) was added slowly to a solution of trifluoroacetic anhydride (0.735 g, 3.5 mmol) in dichloromethane (50 mL) at −78 °C and stirred for 1 h. Solid urethane (0.405 g, 4.55 mmol) was added and stirred for an additional 2 h at −78 °C, at which point the solution was allowed to warm slowly to room temperature and quenched with ice−water. The solution was then washed with aqueous sodium bicarbonate, dried, filtered, and then evaporated to give the crude product. The crude product was purified by column chromatography with 90:10 dichloromethane to ethyl acetate to give 0.17 g of **6** as an off-white solid in 37% yield. Method B began with the synthesis of *N-p*-tosyldibenzothiophene sulfilimine following a literature procedure.[45] *N-p*-Tosyldibenzothiophene sulfilimine (1.0 g, 2.8 mM) was then dissolved in 1 mL of concentrated sulfuric acid (95%) at room temperature for approximately 2 h, and the resulting solution was poured into 100 mL of cold diethyl ether. After removal of solvent, the oil mixture was dissolved in 100 mL of chloroform, washed with ammonium hydroxide (2×), followed by water (5×), and dried with sodium sulfate, and the solvent was removed. The resulting white solid was then dissolved in 50 mL of benzene, to which diethyl pyrocarbonate (0.45 g, 2.8 mmol) was added. The solution was allowed to stir for 1 h, and the benzene was then evaporated; the residue was dissolved in 50 mL of dichloromethane, washed with water (5×), dried with sodium sulfate, and the solvent was removed. The residue was chromatographed on silica gel using 10% ethyl acetate/hexane as an eluent to give 0.38 g (50% yield) of **6**. ^{1}H NMR ($CDCl_3$) δ 8.02 (d, J = 7.8 Hz, 2H), 7.90 (d, J = 7.8 Hz, 2H), 7.65 (t, J = 7.7 Hz, 2H), 7.53 (t, J = 7.7 Hz, 2H), 4.10 (q, J = 7.1 Hz, 2H), 1.20 (t, J = 7.1 Hz, 3 H). ^{13}C NMR ($CDCl_3$) δ 165.8, 138.8, 138.1, 132.5, 129.9, 127.6, 122.3, 62.1, 14.7. HR-MS (FAB): m/z found = 272.07309 (MH^+); calcd for $C_{15}H_{14}NO_2S$ 272.07453 (MH^+).

*N-t-Butyloxycarbonyl Dibenzothiophene Sulfilimine (**7**).* The compound was prepared following procedures similar to those used for the synthesis of sulfilimine **6**, where either di-*t*-butyldicarbonate or *t*-butyl carbamate was used in place of diethyl pyrocarbonate or urethane, respectively. Chromatographic purification resulted in 0.30 g of a white solid, 50% yield. ^{1}H NMR ($CDCl_3$) δ 8.03 (d, J = 7.9 Hz, 2H), 7.63 (d, J = 7.8 Hz, 2H), 7.51 (t, J = 7.8 Hz, 2H), 1.43 (s, 9 H). ^{13}C NMR ($CDCl_3$) δ 165.4, 139.2, 138.1, 132.4, 129.8, 127.8, 122.3, 79.6, 28.4. HR-MS (FAB): m/z found = 300.10546 (MH^+); calcd for $C_{17}H_{18}NO_2S$ 300.10583 (MH^+).

Steady-State Photolysis of Oxycarbonylnitrene Precursors 6 and 7. Photolysis of 12 mM solutions of precursors **6** and **7** in deuterated solvent (dichloromethane or acetonitrile) was performed in a photochemical reactor (254 nm). Following 4 h of photolysis, samples were analyzed by ^{1}H NMR spectroscopy. Yields of observed products are reported relative to dibenzothiophene.

DOI: 10.1021/acs.joc.6b00949
J. Org. Chem. 2016, 81, 6320−6328

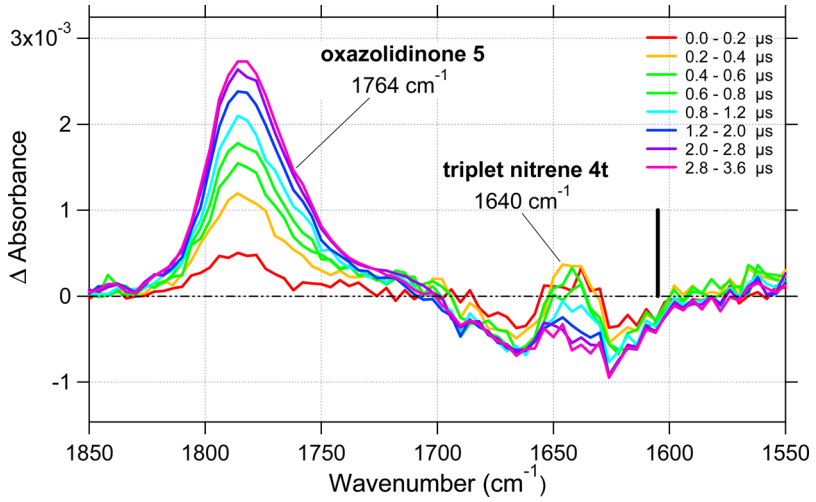

Figure 13. TRIR difference spectra averaged over the indicated time scales following 266 nm laser photolysis of sulfilimine **7** (3 mM) in argon-saturated Freon-113. The black bar reflects the B3LYP/6-31G(d) calculated frequency of *syn*-triplet *t*-butyloxycarbonylnitrene (*syn*-**4t**).

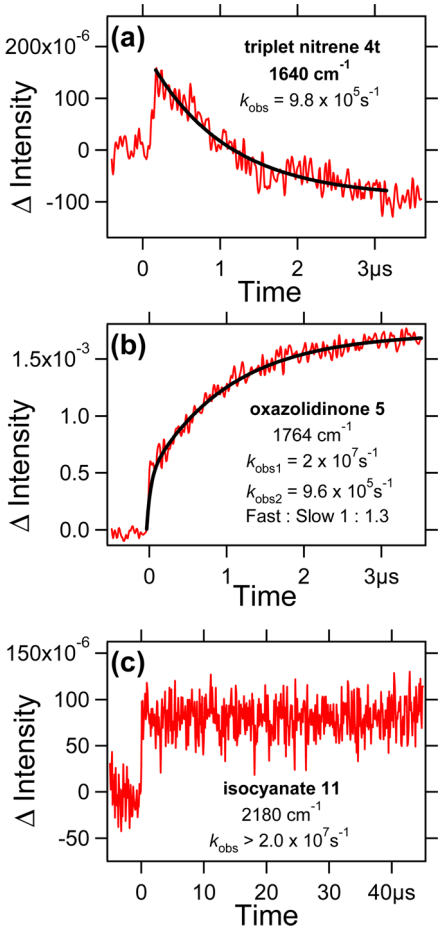

Figure 14. Kinetic traces observed following 266 nm laser photolysis of sulfilimine **7** in argon-saturated Freon-113 at (a) 1640 cm^{-1} from −0.4 to 3.6 μs, (b) 1764 cm^{-1} from −0.4 to 3.6 μs, and (c) 2180 cm^{-1} from −5 to 45 μs. Black curves are the calculated best fit to a single- or double-exponential function.

Time-Resolved IR Methods. TRIR experiments were conducted (with 16 cm^{-1} spectral resolution) following the method of Hamaguchi and co-workers,[46,47] as has been described previously.[48] Briefly, the broadband output of a $MoSi_2$ IR source is crossed with excitation pulses from a Nd:YAG laser (266 nm, 5 ns, 2 mJ) operating at 15 Hz. Changes in IR intensity are monitored using an ac-coupled mercury/cadmium/tellurium (MCT) photovoltaic IR detector amplified, digitized with an oscilloscope, and collected for data processing. The experiment is conducted in dispersive mode with a TRIR spectrometer.

Scheme 6

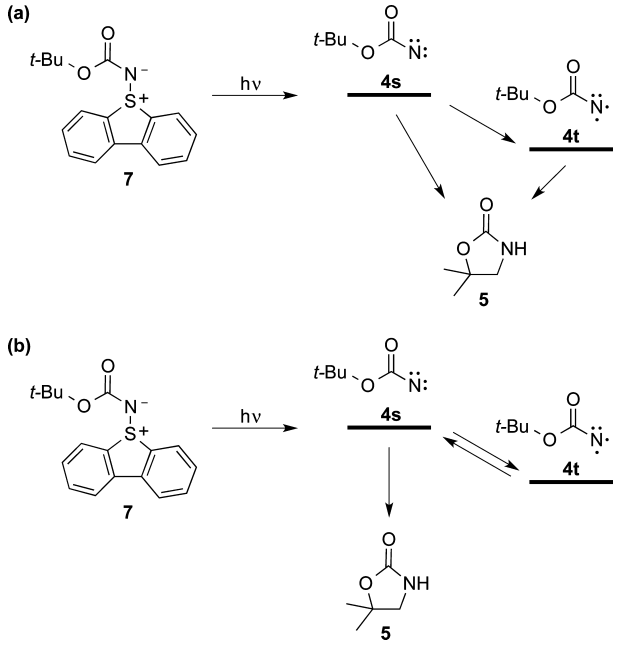

Computational Methods. Calculations were performed with Spartan '14.[49] Geometries were fully optimized at the B3LYP level of theory with the 6-31G(d) basis set. Vibrational frequencies were also calculated to verify minimum energy structures (no imaginary frequencies) or transition states (one imaginary frequency) and to provide zero-point vibrational energy corrections.

■ ASSOCIATED CONTENT

Supporting Information

The Supporting Information is available free of charge on the ACS Publications website at DOI: 10.1021/acs.joc.6b00949.

Spectral data of all final products; additional TRIR data; and computational results including optimized geometries, energies, and vibrational frequencies and intensities (PDF)

DOI: 10.1021/acs.joc.6b00949
J. Org. Chem. 2016, 81, 6320−6328

AUTHOR INFORMATION

Corresponding Author

*E-mail: jtoscano@jhu.edu.

Notes

The authors declare no competing financial interest.

ACKNOWLEDGMENTS

Support of this work by the National Science Foundation (CHE-1213438) is gratefully acknowledged.

REFERENCES

(1) Gritsan, N. P. In *Wiley Series on Reactive Intermediates in Chemistry and Biology, Vol. 6, Nitrenes and Nitrenium Ions*; Falvey, D. E., Gudmundsdottir, A. D., Eds.; John Wiley & Sons, Inc., 2013; pp 481−548.
(2) Lwowski, W.; Mattingly, T. W., Jr. *J. Am. Chem. Soc.* **1965**, *87*, 1947.
(3) Lwowski, W.; Mattingly, T. W. *Tetrahedron Lett.* **1962**, *3*, 277.
(4) Lwowski, W.; McConaghy, J. S. *J. Am. Chem. Soc.* **1965**, *87*, 5490.
(5) McConaghy, J. S.; Lwowski, W. *J. Am. Chem. Soc.* **1967**, *89*, 2357.
(6) Hafner, K.; Kaiser, W.; Puttner, R. *Tetrahedron Lett.* **1964**, *5*, 3953.
(7) Kreher, R.; Bockhorn, G. H. *Angew. Chem.* **1964**, *76*, 681.
(8) Puttner, R.; Hafner, K. *Tetrahedron Lett.* **1964**, *5*, 3119.
(9) Meth-Cohn, O. *Acc. Chem. Res.* **1987**, *20*, 18.
(10) Sigman, M. E.; Autrey, T.; Schuster, G. B. *J. Am. Chem. Soc.* **1988**, *110*, 4297.
(11) Buron, C.; Platz, M. S. *Org. Lett.* **2003**, *5*, 3383.
(12) Murthy, R. S.; Muthukrishnan, S.; Rajam, S.; Mandel, S. M.; Ault, B. S.; Gudmundsdottir, A. D. *J. Photochem. Photobiol., A* **2009**, *201*, 157.
(13) Lwowski, W.; DeMauriac, R.; Mattingly, T. W.; Scheiffele, E. *Tetrahedron Lett.* **1964**, *5*, 3285.
(14) Tisue, G. T.; Linke, S.; Lwowski, W. *J. Am. Chem. Soc.* **1967**, *89*, 6303.
(15) Linke, S.; Tisue, G. T.; Lwowski, W. *J. Am. Chem. Soc.* **1967**, *89*, 6308.
(16) Wilde, R. E.; Srinivasan, T. K. K.; Lwowski, W. *J. Am. Chem. Soc.* **1971**, *93*, 860.
(17) Teles, J. H.; Maier, G. *Chem. Ber.* **1989**, *122*, 745.
(18) Pritchina, E. A.; Gritsan, N. P.; Maltsev, A.; Bally, T.; Autrey, T.; Liu, Y.; Wang, Y.; Toscano, J. P. *Phys. Chem. Chem. Phys.* **2003**, *5*, 1010.
(19) Kubicki, J.; Zhang, Y.; Wang, J.; Luk, H. L.; Peng, H.-L.; Vyas, S.; Platz, M. S. *J. Am. Chem. Soc.* **2009**, *131*, 4212.
(20) Kubicki, J.; Zhang, Y.; Vyas, S.; Burdzinski, G.; Luk, H. L.; Wang, J.; Xue, J.; Peng, H. L.; Pritchina, E. a.; Sliwa, M.; Buntinx, G.; Gritsan, N. P.; Hadad, C. M.; Platz, M. S. *J. Am. Chem. Soc.* **2011**, *133*, 9751.
(21) Vyas, S.; Kubicki, J.; Luk, H. L.; Zhang, Y.; Gritsan, N. P.; Hadad, C. M.; Platz, M. S. *J. Phys. Org. Chem.* **2012**, *25*, 693.
(22) Kubicki, J.; Zhang, Y.; Xue, J.; Ling Luk, H.; Platz, M. *Phys. Chem. Chem. Phys.* **2012**, *14*, 10377.
(23) Wasserman, E. In *Progress in Physical Organic Chemistry*; John Wiley & Sons, Inc., 1971; pp 319−336.
(24) Autrey, T.; Schuster, G. B. *J. Am. Chem. Soc.* **1987**, *109*, 5814.
(25) Gritsan, N. P.; Pritchina, E. A. *Mendeleev Commun.* **2001**, *11*, 94.
(26) Faustov, V.; Baskir, E.; Biryukov, A. *Russ. Chem. Bull.* **2003**, *52*, 2328.
(27) Liu, J.; Mandel, S.; Hadad, C. M.; Platz, M. S. *J. Org. Chem.* **2004**, *69*, 8583.
(28) Pritchina, E. a.; Gritsan, N. P.; Bally, T. *Russ. Chem. Bull.* **2005**, *54*, 525.
(29) Desikan, V.; Liu, Y.; Toscano, J. P.; Jenks, W. S. *J. Org. Chem.* **2008**, *73*, 4398.
(30) Zeng, X.; Beckers, H.; Willner, H.; Grote, D.; Sander, W. *Chem. - Eur. J.* **2011**, *17*, 3977.
(31) Sherman, M. P.; Jenks, W. S. *J. Org. Chem.* **2014**, *79*, 8977.
(32) Sun, H.; Zhu, B.; Wu, Z.; Zeng, X.; Beckers, H.; Jenks, W. S. *J. Org. Chem.* **2015**, *80*, 2006.
(33) Desikan, V.; Liu, Y.; Toscano, J. P.; Jenks, W. S. *J. Org. Chem.* **2007**, *72*, 6848.
(34) Fujita, T.; Kamiyama, H.; Osawa, Y.; Kawaguchi, H.; Kim, B. J.; Tatami, A.; Kawashima, W.; Maeda, T.; Nakanishi, A.; Morita, H. *Tetrahedron* **2007**, *63*, 7708.
(35) Fujita, T.; Maeda, T.; Kim, B. J.; Tatami, A.; Miyamoto, D.; Kawaguchi, H.; Tsuchiya, N.; Yoshida, M.; Kawashima, W.; Morita, H. *J. Sulfur Chem.* **2008**, *29*, 459.
(36) Morita, H.; Tatami, A.; Maeda, T.; Kim, B. J.; Kawashima, W.; Yoshimura, T.; Abe, H.; Akasaka, T. *J. Org. Chem.* **2008**, *73*, 7159.
(37) Scott, A. P.; Radom, L. *J. Phys. Chem.* **1996**, *100*, 16502.
(38) Liu, Y.; Evans, A. S.; Toscano, J. P. *Phys. Chem. Chem. Phys.* **2012**, *14*, 10438.
(39) Desikan, V.; Liu, Y.; Toscano, J. P.; Jenks, W. S. *J. Org. Chem.* **2008**, *73*, 4398.
(40) Pandey, R. K.; Dagade, S. P.; Dongare, M. K.; Kumar, P. *Synth. Commun.* **2003**, *33*, 4019.
(41) Huard, K.; Lebel, H. *Chem. - Eur. J.* **2008**, *14*, 6222.
(42) Geise, C. M.; Wang, Y.; Mykhaylova, O.; Frink, B. T.; Toscano, J. P.; Hadad, C. M. *J. Org. Chem.* **2002**, *67*, 3079.
(43) Wang, Y.; Hadad, C. M.; Toscano, J. P. *J. Am. Chem. Soc.* **2002**, *124*, 1761.
(44) Nakayama, J.; Otani, T.; Sugihara, Y.; Sano, Y.; Ishii, A.; Sakamoto, A. *Heteroat. Chem.* **2001**, *12*, 333.
(45) Svoronos, P.; Horak, V. *Synthesis* **1979**, *1979*, 596.
(46) Iwata, K.; Hamaguchi, H. *Appl. Spectrosc.* **1990**, *44*, 1431.
(47) Yuzawa, T.; Kato, C.; George, M. W.; Hamaguchi, H. *Appl. Spectrosc.* **1994**, *48*, 684.
(48) Wang, Y. H.; Yuzawa, T.; Hamaguchi, H.; Toscano, J. P. *J. Am. Chem. Soc.* **1999**, *121*, 2875.
(49) Shao, Y.; Molnar, L. F.; Jung, Y.; Kussmann, J.; Ochsenfeld, C.; Brown, S. T.; Gilbert, A. T. B.; Slipchenko, L. V.; Levchenko, S. V.; O'Neill, D. P.; DiStasio, R. A., Jr; Lochan, R. C.; Wang, T.; Beran, G. J. O.; Besley, N. A.; Herbert, J. M.; Yeh Lin, C.; Van Voorhis, T.; Hung Chien, S.; Sodt, A.; Steele, R. P.; Rassolov, V. A.; Maslen, P. E.; Korambath, P. P.; Adamson, R. D.; Austin, B.; Baker, J.; Byrd, E. F. C.; Dachsel, H.; Doerksen, R. J.; Dreuw, A.; Dunietz, B. D.; Dutoi, A. D.; Furlani, T. R.; Gwaltney, S. R.; Heyden, A.; Hirata, S.; Hsu, C.-P.; Kedziora, G.; Khalliulin, R. Z.; Klunzinger, P.; Lee, A. M.; Lee, M. S.; Liang, W.; Lotan, I.; Nair, N.; Peters, B.; Proynov, E. I.; Pieniazek, P. A.; Min Rhee, Y.; Ritchie, J.; Rosta, E.; David Sherrill, C.; Simmonett, A. C.; Subotnik, J. E.; Lee Woodcock, H., III; Zhang, W.; Bell, A. T.; Chakraborty, A. K.; Chipman, D. M.; Keil, F. J.; Warshel, A.; Hehre, W. J.; Schaefer, H. F., III; Kong, J.; Krylov, A. I.; Gill, P. M. W.; Head-Gordon, M. *Phys. Chem. Chem. Phys.* **2006**, *8*, 3172.

DOI: 10.1021/acs.joc.6b00949
J. Org. Chem. 2016, 81, 6320−6328